J|A|C|S
ARTICLES
Published on Web 02/16/2002

Remarkable Variations in the Luminescence of Frozen Solutions of [Au{C(NHMe)$_2$}$_2$](PF$_6$)·0.5(Acetone). Structural and Spectroscopic Studies of the Effects of Anions and Solvents on Gold(I) Carbene Complexes

Rochelle L. White-Morris, Marilyn M. Olmstead, Feilong Jiang, Dino S. Tinti, and Alan L. Balch*

Contribution from the Department of Chemistry, University of California, Davis, California 95616

Received October 22, 2001

Abstract: The unusual luminescence behavior of the two-coordinate gold(I) carbene complex, [Au{C(NHMe)$_2$}$_2$](PF$_6$)·0.5(acetone), is reported. Upon freezing in a liquid N_2 bath, the colorless, nonluminescent solutions of [Au{C(NHMe)$_2$}$_2$](PF$_6$)·0.5(acetone) become intensely luminescent. Strikingly, the colors of the emission differ in different solvents and appear only after the solvent has frozen. Solid [Au{C(NHMe)$_2$}$_2$](PF$_6$)·0.5(acetone) is also luminescent, and the luminescence is attributed to the formation of extended chains of gold(I) centers that are connected through aurophilic attractions. Crystallographic studies of [Au{C(NHMe)$_2$}$_2$](PF$_6$)·0.5(acetone) and [Au{C(NHMe)$_2$}$_2$](BF$_4$), which is also luminescent, reveal that both involve extended chains of cations and that the anions are hydrogen bonded to the cations through cation N−H groups. However, these chains differ in the Au···Au separations in each and in the carbene ligand orientations. In contrast, [Au{C(NMe$_2$)(NHMe)}$_2$](PF$_6$) forms a colorless, nonluminescent solid, and in that solid there are no Au···Au interactions, a factor which supports the contention that aggregated species are responsible for the luminescence of [Au{C(NHMe)$_2$}$_2$](PF$_6$)·0.5(acetone) in the solid state and in frozen solutions.

Introduction

Gold(I) complexes typically are colorless, two-coordinate species that readily self-associate to form dimers, trimers, and extended chains connected by Au···Au contacts that are less than the van der Waals separation of ca. 3.6 Å.[1−3] Attractive interactions between closed-shell Au(I) centers are important in determining the solid-state structures of many gold(I) complexes[4,5] and contribute to the properties of such complexes in solution as well.[6−8] Theoretical studies have shown that this weakly bonding interaction is the result of correlation effects that are enhanced by relativistic effects.[9−12] Experimental studies of rotational barriers have shown that the strength of this attractive interaction is comparable to hydrogen bonding, ca. 7−11 kcal/mol.[6,7] Such aurophilic interactions have been shown to be sufficiently strong to persist in solution and to play a role in guiding a chemical reaction.[8,13]

Many gold complexes display intense luminescence, and in some cases the luminescence is correlated with aggregation through aurophilic interactions.[14−16] In these cases, the spectroscopic features result from the overlap of filled d orbitals and empty p orbitals on gold much like that seen for d^8 metal complexes: $[Rh^{I}(CNR)_4]_n^{n+}$,[17,18] $[Pt^{II}(CN)_4]_n^{2n-}$,[19] and $[Pt_2(\mu\text{-}P_2O_5H_2)_4]^{4-}$.[20,21]

The absorption and luminescence features of gold complexes and related transition metal complexes make them suitable for sensor applications. Eisenberg, Gysling, and co-workers have

(1) Schmidbaur, H. *Gold: Progress in Chemistry, Biochemistry, and Technology*; Wiley: New York, 1999.
(2) Grohmann, A.; Schmidbaur, H. In *Comprehensive Organometallic Chemistry II*; Abel, E. W., Stone, F. G. A., Wilkinson, G., Eds.; Elsevier: Oxford, 1995; Vol. 3, p 1.
(3) Puddephatt, R. J. In *Comprehensive Coordination Chemistry*; Wilkinson, G., Gillard, R. D., McCleverty, J. A., Eds.; Pergamon Press: Oxford, 1987; Vol. 5, p 861.
(4) Jones, P. G. *Gold Bull.* **1986**, *19*, 46−54; **1983**, *16*, 114−120; **1981**, *14*, 159−168; **1981**, *14*, 102.
(5) Pathaneni, S. S.; Desiraju, G. R. *J. Chem. Soc., Dalton Trans.* **1993**, 319.
(6) Schmidbaur, H.; Graf, W.; Müller, G. *Angew. Chem., Int. Ed. Engl.* **1988**, *27*, 417.
(7) Harwell, D. E.; Mortimer, M. D.; Knobler, C. B.; Anet, F. A. L.; Hawthorne, M. F. *J. Am. Chem. Soc.* **1996**, *118*, 2679.
(8) Balch, A. L.; Fung, E. Y.; Olmstead, M. M. *J. Am. Chem. Soc.* **1990**, *112*, 5181.
(9) Pyykkö, P.; Runeberg, N.; Mendizabal, F. *Chem.-Eur. J.* **1997**, *3*, 1451.
(10) Pyykkö, P.; Mendizabal, F. *Chem.-Eur. J.* **1997**, *3*, 1458.
(11) Pyykkö, P. *Chem. Rev.* **1997**, *97*, 597.
(12) Pyykkö, P.; Li, J.; Runeberg, N. *Chem. Phys. Lett.* **1994**, *218*, 133.
(13) Zank, J.; Schier, A.; Schmidbaur, H. *J. Chem. Soc., Dalton Trans.* **1998**, 323.
(14) Forward, J. M.; Fackler, J. P., Jr.; Assefa, Z. In *Optoelectronic Properties of Inorganic Compounds*; Roundhill, D. M., Fackler, J. P., Jr., Eds.; Plenum Press: New York, 1999; p 195.
(15) Yam, V. W. W.; Lo, K. K. W. *Chem. Soc. Rev.* **1999**, *28*, 323.
(16) Leung, K. H.; Phillips, D. L.; Tse, M. C.; Che, C. M.; Miskowski, V. M. *J. Am. Chem. Soc.* **1999**, *121*, 4799.
(17) Mann, K. R.; Gordon, J. G., II; Gray, H. B. *J. Am. Chem. Soc.* **1975**, *97*, 3553.
(18) Balch, A. L.; Olmstead, M. M. *J. Am. Chem. Soc.* **1976**, *98*, 2354.
(19) Williams, J. M.; Schultz, A. J.; Underhill, A. E.; Caneiro, K. In *Extended Linear Chain Complexes*; Miller, J. S., Ed.; Plenum Press: New York, 1982; Vol. 1, p 73.
(20) Roundhill, D. M.; Gray, H. B.; Che, C. M. *Acc. Chem. Res.* **1989**, *22*, 55.
(21) Zipp, A. P. *Coord. Chem. Rev.* **1988**, *84*, 47.

found that the binuclear dithiocarbamate complex, $Au^{I}_2\{S_2CN(n\text{-pentyl})_2\}_2$, crystallizes in a colorless form as well-separated dimer molecules, but forms an orange, luminescent form when exposed to the vapor of aprotic organic solvents.[22] The orange form has been crystallized from dimethyl sulfoxide and involves an extended chain of the dimers with inter- and intramolecular Au···Au separations of 2.96 and 2.77 Å. However, it is not clear how the solvent facilitates the formation of the extended structure of the orange form. Mann and co-workers have discovered that complexes of the type $[Pt(CNAr)_4][M(CN)_4]$ form columns in the solid state with extended ···Pt···M···Pt···M··· interactions.[23−27] These complexes display vapor-induced color changes that result from absorption of solvent molecules, which appear to form hydrogen bonds with the cyano ligands. Patterson and co-workers have shown that the simple $[Au(CN)_2]^-$ and $[Ag(CN)_2]^-$ ions aggregate under a variety of conditions and that the aggregated forms show alteration of their luminescence.[28−30] Yam and co-workers developed a sensor for potassium ions that operates through enhancement of Au···Au contacts.[31]

The crystalline gold trimer $\{Au_3(MeN{=}COMe)_3\}$,[32] whose molecular structure is shown below, displays a novel physical property, solvoluminescence.[33,34] After irradiation with near UV light, crystals of $\{Au_3(MeN{=}COMe)_3\}$ show a long-lived yellow photoluminescence that is readily detected in a dark room by the human eye for tens of seconds after irradiation ceases. Addition of dichloromethane or chloroform to such previously irradiated crystals produces a bright burst of yellow light. Since the intensity of this emission is greatest for those liquids that are good solvents for $\{Au_3(MeN{=}COMe)_3\}$, the phenomenon has been termed solvoluminescence. The light produced by solvoluminescence has been shown to correlate with the emission characteristics of the solid rather than those of the molecule in solution. Consequently, the solid-state structure of $\{Au_3(MeN{=}COMe)_3\}$, which involves prismatic stacking of these triangular molecules into extended stacks, is crucial to the occurrence of solvoluminescence.[32,35]

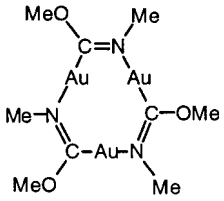

$\{Au_3(MeN{=}COMe)_3\}$

Here we describe the unusual luminescence behavior of some simple gold(I) complexes with two carbene ligands, which are shown in Chart 1. These complexes are readily prepared by the addition of methylamine (to give $[Au\{C(NHMe)_2\}_2](PF_6)\cdot 0.5$(acetone), **1**, and $[Au\{C(NHMe)_2\}_2](BF_4)$, **2**) or dimethylamine (to give $[Au\{C(NMe_2)(NHMe)\}_2](PF_6)$, **3**) to a mixture of chloroauric acid and methyl isocyanide in water as described earlier.[32]

Chart 1

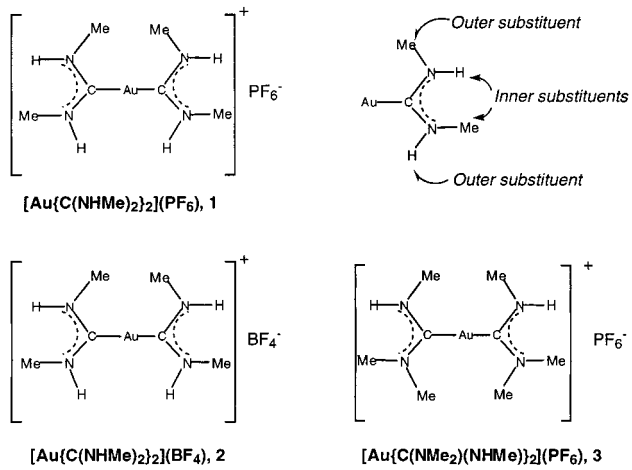

$[Au\{C(NHMe)_2\}_2](PF_6)$, 1

$[Au\{C(NHMe)_2\}_2](BF_4)$, 2

$[Au\{C(NMe_2)(NHMe)\}_2](PF_6)$, 3

Results

Unusual Luminescence from $[Au\{C(NHMe)_2\}_2](PF_6)\cdot 0.5$(Acetone), 1. The colorless complex $[Au\{C(NHMe)_2\}_2](PF_6)\cdot 0.5$(acetone), **1**,[32] displays unique photoluminescence behavior. In the solid state at room temperature, crystalline $[Au\{C(NHMe)_2\}_2](PF_6)\cdot 0.5$(acetone) produces a green-blue luminescence (λ_{max}, 460 nm) when irradiated with an UV lamp. The emission and excitation spectra of the solid at 300 K are shown in trace A of Figure 1. Trace B of this figure shows the time-resolved emission spectra at 300 K, while trace C shows the emission spectrum at 77 K. The emission spectra consist of two bands whose maxima red shift by ca. 1200 cm^{-1} upon lowering the temperature from 300 to 77 K. The higher energy band is short-lived (<100 ns). The lower energy decays nearly exponentially with a lifetime of 1.9 μs at 300 K and 2.4 μs at 77 K. The lower energy band is more intense in the spectra with continuous excitation at both 300 and 77 K.

When dissolved in solvents such as acetone, pyridine, dimethyl sulfoxide, dimethylformamide, and acetonitrile, this salt produces colorless solutions (λ_{max}, 210 nm; ϵ, 13 900 M^{-1} cm^{-1} in acetonitrile solution at 298 K) that are not luminescent. However, upon freezing in a liquid N_2 bath, these solutions become intensely luminescent. Strikingly, the colors of the emission differ in different solvents as seen in Figure 2. The frozen acetonitrile solution produces a green-yellow luminescence, with dimethyl sulfoxide and pyridine the emission is different shades of blue, with acetone it is orange, but with dimethylformamide no luminescence is observed. The process is entirely reversible; warming the samples results in the loss

(22) Mansour, M. A.; Connick, W. B.; Lachicotte, R. J.; Gysling, H. J.; Eisenberg, R. *J. Am. Chem. Soc.* **1998**, *120*, 1329.
(23) Exstrom, C. L.; Sowa, J. R.; Daws, C. A.; Janzen, D.; Mann, K. R.; Moore, G. A.; Stewart, F. F. *Chem. Mater.* **1995**, *7*, 15.
(24) Daws, C. A.; Exstrom, C. L.; Sowa, J. R.; Mann, K. R. *Chem. Mater.* **1997**, *9*, 363.
(25) Kunugi, Y.; Miller, L. L.; Mann, K. R.; Pomije, M. K. *Chem. Mater.* **1998**, *10*, 1487.
(26) Buss, C. E.; Anderson, C. E.; Pomije, M. K.; Lutz, C. M.; Britton, D.; Mann, K. R. *J. Am. Chem. Soc.* **1998**, *120*, 7783.
(27) Drew, S. M.; Janzen, D. E.; Buss, C. E.; MacEwan, D. I.; Dublin, K. M.; Mann, K. R. *J. Am. Chem. Soc.* **2001**, *123*, 8414.
(28) Rawashdeh-Omary, M. A.; Omary, M. A.; Patterson, H. H. *J. Am. Chem. Soc.* **2000**, *122*, 10371.
(29) Rawashdeh-Omary, M. A.; Omary, M. A.; Shankle, G. E.; Patterson, H. H. *J. Phys. Chem. B* **2000**, *104*, 6143.
(30) Omary, M. A.; Patterson, H. H. *J. Am. Chem. Soc.* **1998**, *120*, 7696.
(31) Yam, V. W. W.; Li, C. K.; Chan, C. L. *Angew. Chem., Int. Ed.* **1998**, *37*, 2857.
(32) Parks, J. E.; Balch, A. L. *J. Organomet. Chem.* **1974**, *71*, 453.
(33) Vickery, J. C.; Olmstead, M. M.; Fung, E. Y.; Balch, A. L. *Angew. Chem., Int. Ed. Engl.* **1997**, *36*, 1179.
(34) Fung, E. Y.; Olmstead, M. M.; Vickery, J. C.; Balch, A. L. *Coord. Chem. Rev.* **1998**, *171*, 151.
(35) Olmstead, M. M.; Jiang, F.; Attar, S.; Balch, A. L. *J. Am. Chem. Soc.* **2001**, *123*, 3260.

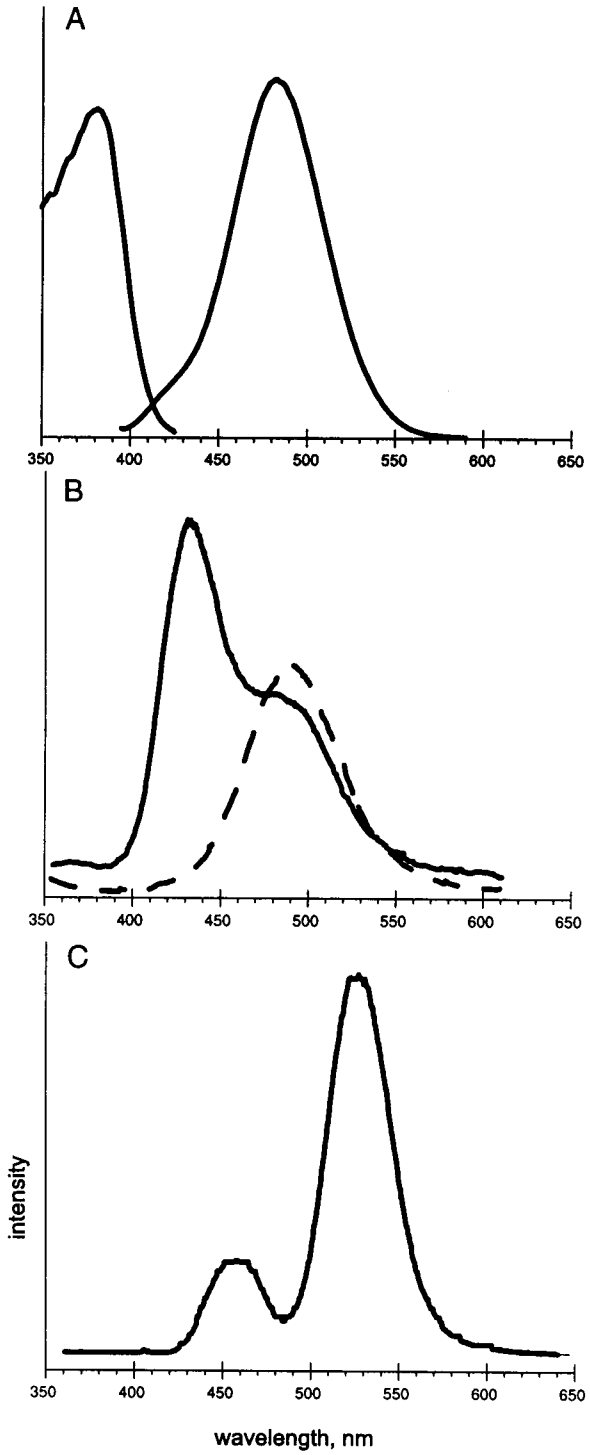

Figure 1. Emission spectra of polycrystalline [Au{C(NHMe)$_2$}$_2$](PF$_6$)·0.5(acetone), **1**. A, Emission ($\lambda_{excitation}$, 383 nm) and excitation ($\lambda_{emission}$, 482 nm) spectra at 300 K. B, Time-resolved emission spectra at 300 K; solid line emission acquired within 50 ns of a 337 nm laser pulse; dotted line emission acquired 200 ns after the laser pulse. C, Emission ($\lambda_{excitation}$, 365 nm) spectrum at 77 K.

of the luminescence, while refreezing restores the colors. These colors are produced at different temperatures as each solvent freezes. Figure 3 shows the emission spectra obtained from frozen solutions of the complex at 77 K in acetone, acetonitrile, dimethyl sulfoxide, and pyridine.

The variation in luminescence is affected by the concentration of [Au{C(NHMe)$_2$}$_2$](PF$_6$)·0.5(acetone) in solution before cooling. The data shown in Figure 3 were obtained from frozen solutions with an initial 6 mM concentration of [Au{C(NHMe)$_2$}$_2$](PF$_6$)·0.5(acetone). As seen in Figure 4, solutions with only a 0.06 mM concentration of the complex (except dimethylformamide which is nonluminescent as before) produce luminescence with two major bands that are very similar to that of crystalline [Au{C(NHMe)$_2$}$_2$](PF$_6$)·0.5(acetone).

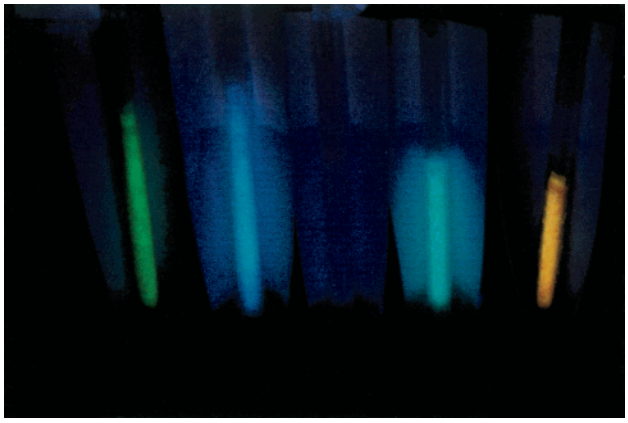

Figure 2. Photograph of the luminescence from 6 mM solutions of [Au{C(NHMe)$_2$}$_2$](PF$_6$)·0.5(acetone), **1**, that have been frozen in a liquid nitrogen bath. From left to right the solvents are acetonitrile, dimethyl sulfoxide, dimethylformamide, pyridine, and acetone.

Table 1. Selected Interatomic Distances and Angles in Gold Carbene Cations

	[Au{C(NHMe)$_2$}$_2$](PF$_6$)·0.5(acetone), **1**	[Au{C(NHMe)$_2$}$_2$](BF$_4$), **2**	[Au{C(NMe$_2$)(NHMe)}$_2$](PF$_6$), **3**
	distances (Å)		
Au−C	2.039(3)	2.041(3)	2.050(3)
C1−N1	1.326(4)	1.330(3)	1.331(3)
C1−N2	1.333(4)	1.332(3)	1.336(4)
Au···Au	3.1882(1)	3.4615(2)	
	angles (deg)		
C−Au−C	180	178.42(12)	180
C−Au−Au′	90	75.79(7)	
C−Au−Au′		104.05(7)	
Au−C1−N1	124.3(2)	121.20(17)	122.68(19)
Au−C1−N2	119.3(2)	121.40(16)	120.66(19)
N1−C1−N2	116.4(3)	117.4(2)	116.7(2)
Au···Au···Au	180	169.22(1)	

Crystal Structure of [Au{C(NHMe)$_2$}$_2$](PF$_6$)·0.5(Acetone). The structure of a portion of this solid is shown in Figure 5. Selected bond distances within an individual cation are given in Table 1. The cation consists of a gold(I) center coordinated by two diaminocarbene ligands in a linear fashion. The atoms of each cation (excluding the hydrogen atoms of the methyl groups) sit on a crystallographic mirror plane. Consequently, the two ligands are coplanar, and the carbon and nitrogen atoms have planar bonding. The dimensions within this cation are consistent with parameters seen for other related two-coordinate complexes such as [bis(1,3-($C_{16}H_{33}$)benzimidazol-2-ylidene)-gold(I)]bromide, where the Au−C distance is 2.03(2) Å,[36] and [Au{C(OMe)(NMeH)}$_2$]$^+$, where the Au−C distances in three different salts fall in the range from 2.025(4) to 2.031(3) Å.[37]

The gold cations in [Au{C(NHMe)$_2$}$_2$](PF$_6$)·0.5(acetone), **1**, are organized into linear stacks along the crystallographic 4_2

(36) Lee, K. M.; Lee, C. K.; Lin, I. J. B. *Angew. Chem., Int. Ed. Engl.* **1997**, *36*, 1850.
(37) Jiang, F.; Olmstead, M. M.; Balch, A. L. *J. Chem. Soc., Dalton Trans.* **2000**, 4098.

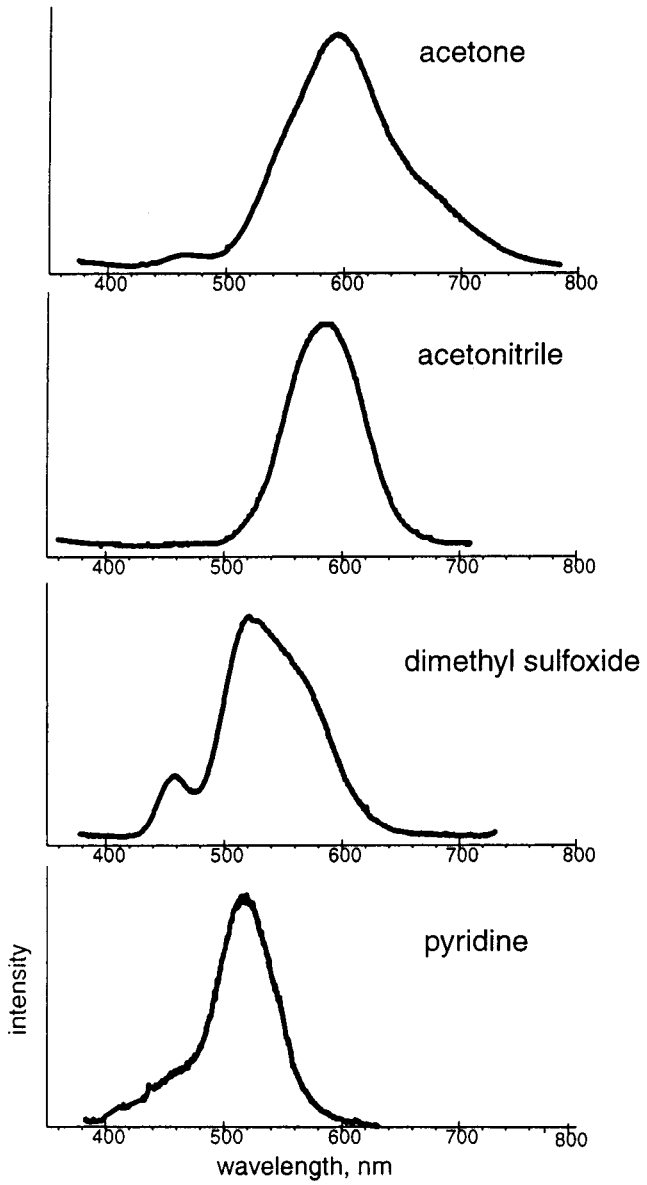

Figure 3. The emission spectra obtained from 6 mM solutions of [Au{C(NHMe)$_2$}$_2$](PF$_6$)·0.5(acetone), **1**, in the following: A, acetone (λ_{max} 591 nm); B, acetonitrile (λ_{max} 586 nm); C, dimethyl sulfoxide (λ_{max} 459, 523, 570sh nm); and D, pyridine, (λ_{max} 511 nm) frozen at 77 K.

screw axis. The Au···Au distance is 3.1882(1) Å, which is in the range where aurophilic attractions occur. Within the stacks the carbene ligands are staggered. Significantly, the ligands of adjacent cations are linked through hydrogen bonds with the hexafluorophosphate anion. These hydrogen bonds involve the inner N−H of one ligand, which is bonded to a fluorine atom of a hexafluorophosphate ion, and the outer N−H of another, which is bonded to another fluorine atom of the same hexafluorophosphate ion.

As seen in Figure 6, which shows the unit cell of the solid, the acetone molecules reside in channels between four stacks of cations and do not coordinate to gold of the cations or hydrogen bond to the carbene ligands. The acetone molecules are disordered and are situated at a site of *mmm* symmetry.

Luminescence from [Au{C(NHMe)$_2$}$_2$](BF$_4$), 2. Colorless crystals of [Au{C(NHMe)$_2$}$_2$](BF$_4$), **2**, produce a blue luminescence under UV irradiation. The emission and excitation

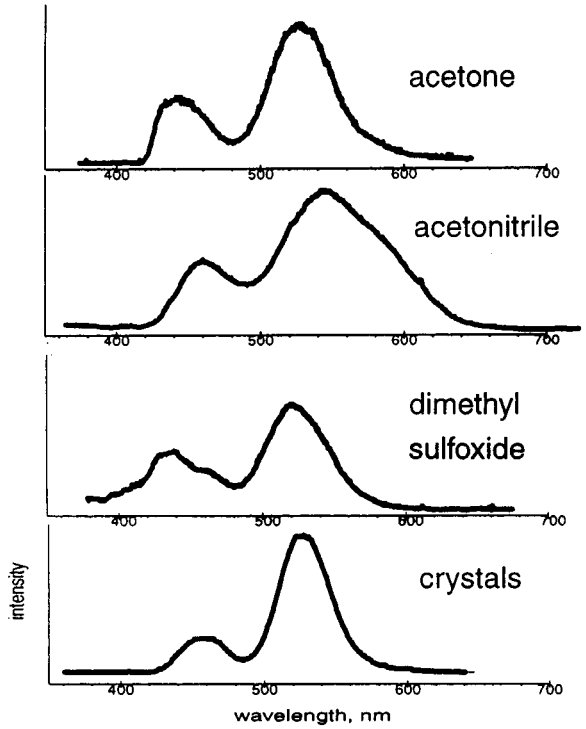

Figure 4. The emission spectra obtained from 0.06 mM solutions of [Au{C(NHMe)$_2$}$_2$](PF$_6$)·0.5(acetone), **1**, in acetone, dimethyl sulfoxide, and acetonitrile frozen at 77 K and from crystalline [Au{C(NHMe)$_2$}$_2$](PF$_6$)·0.5(acetone), **1**.

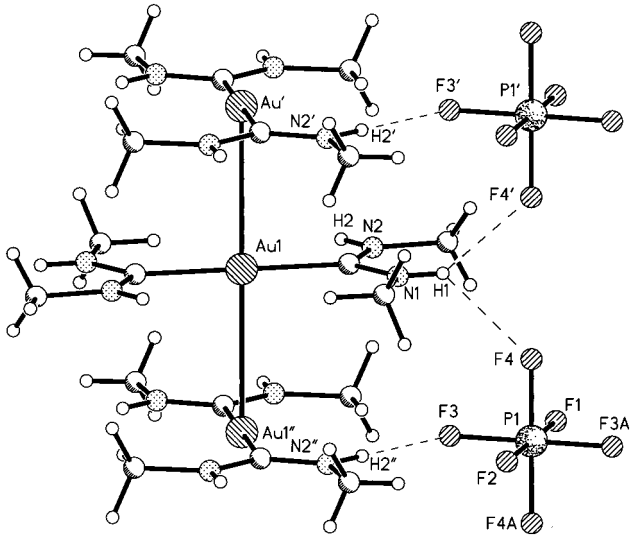

Figure 5. A portion of the structure of crystalline [Au{C(NHMe)$_2$}$_2$](PF$_6$)·0.5(acetone), **1**, which emphasizes aurophilic interactions and the hydrogen-bonding interactions between two cations and a hexafluorophosphate anion.

spectra of the solid at 300 K are shown in trace A of Figure 7, along with the time-resolved emission at 300 K (trace B) and the emission spectrum at 77 K (trace C). The emission of this salt shows similar features and properties to those of [Au{C(NHMe)$_2$}$_2$](PF$_6$)·0.5(acetone), **1**. The spectra consist of two bands which red shift (by ca. 500−1000 cm^{-1}) with decreasing temperature. The higher energy band decays within 100 ns, while the lower energy band shows a lifetime of 1.5 μs at 300 K and 2.1 μs at 77 K. The lower energy band is more intense than the high energy band in the spectrum seen in trace C of Figure 7, but less so than in the hexafluorophosphate salt **1** as

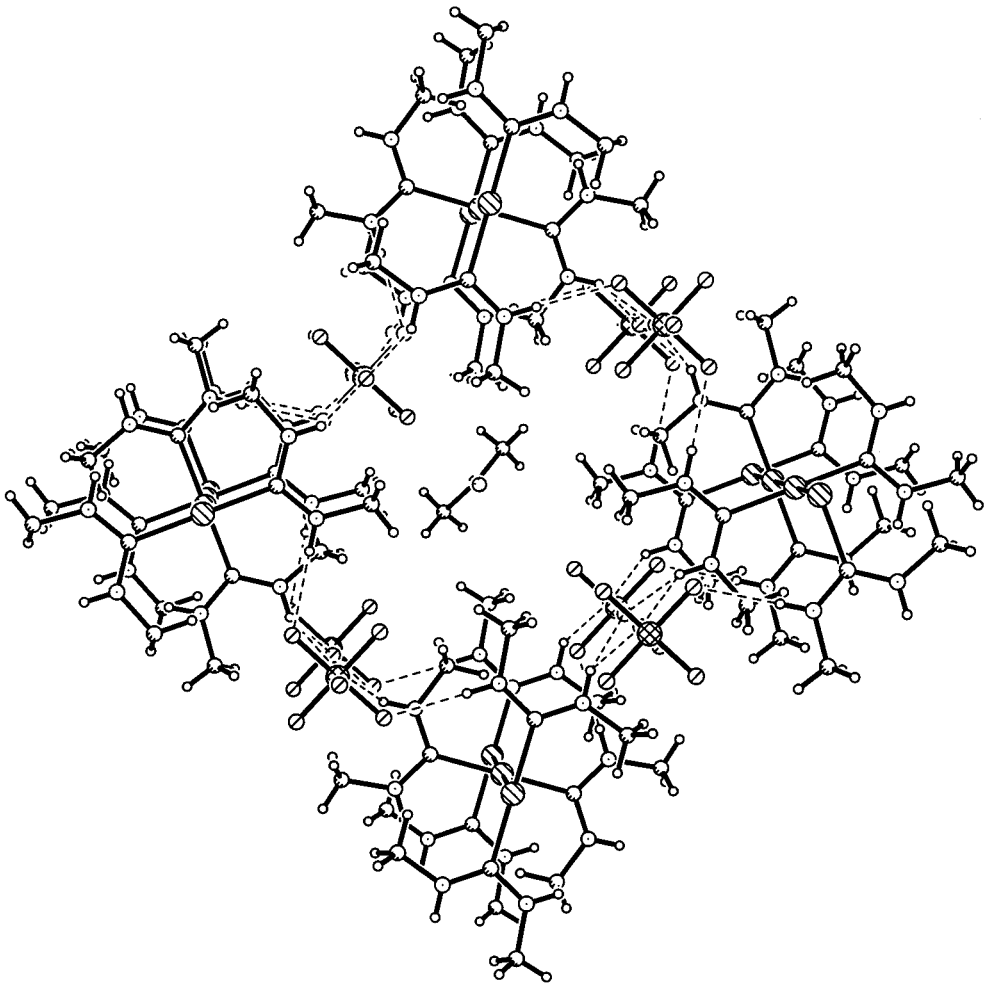

Figure 6. A view of the structure of crystalline [Au{C(NHMe)$_2$}$_2$](PF$_6$)·0.5(acetone), **1**, which shows the location of the acetone molecules between the columns of gold-containing cations.

seen in trace C of Figure 1. Both bands in [Au{C(NHMe)$_2$}$_2$]-(BF$_4$), **2**, are blue-shifted (by ca. 500−1000 cm^{-1}) relative to the bands of [Au{C(NHMe)$_2$}$_2$](PF$_6$)·0.5(acetone), **1**, at both 300 and 77 K.

Solutions of [Au{C(NHMe)$_2$}$_2$](BF$_4$), **2**, in acetone, pyridine, dimethyl sulfoxide, and acetonitrile are not luminescent at room temperature, but upon freezing, these solutions become luminescent. Figure 8 shows luminescence spectra obtained from frozen 6 mM solutions of [Au{C(NHMe)$_2$}$_2$](BF$_4$), **2**, in acetone, acetonitrile, and dimethyl sulfoxide at 77 K, as well as the spectrum of the crystalline solid. The spectra from the different solvents show some variation but less so than that seen in Figure 3 and more in line with the spectra shown in Figure 4.

Crystal Structure of [Au{C(NHMe)$_2$}$_2$](BF$_4$), 2. Figures 9−11 show portions of the structure of this solid. The gold and boron atoms sit at sites of two-fold rotational symmetry. The dimensions within the cation are similar to those of [Au-{C(NHMe)$_2$}$_2$](PF$_6$)·0.5(acetone), **1**, as seen in Table 1, but structures of the cations in the two salts differ in the relative ligand orientations. In both salts the cations are planar, but in [Au{C(NHMe)$_2$}$_2$](BF$_4$), **2**, the two ligands are arranged so that the outer methyl groups face one another as do the outer N−H groups. As seen in Figure 9, this orientation of the carbene ligands allows both N−H groups of one cation to form hydrogen bonds to two different fluorine atoms of a common tetrafluoroborate anion. In contrast, in [Au{C(NHMe)$_2$}$_2$](PF$_6$)·0.5-(acetone), **1**, the ligands are rotated by 180° so that the outer methyl groups face the outer N−H groups of the opposite ligand. Figure 9 also shows that each tetrafluoroborate anion is hydrogen bonded to the inner N−H groups of two other cations to form a network of interconnected cations and anions with each cation hydrogen bonded to two anions and each anion hydrogen bonded to two cations. The entire cation, with the exception of the methyl hydrogen atoms, is nearly planar with both ligands coplanar. The out-of-plane displacements of the various atoms are Au 0.000, C1 0.001, C2 0.125, C3 −0.58, N1 0.29, N2 −0.34, C1A −0.001, C2A −0.125, C3A 0.58, NA1 −0.29, N2A 0.034 Å.

As seen in the stereoview of the unit cell shown in Figure 10 and in Figure 11, which shows the cationic interactions, the individual cations are arranged so that they form offset stacks in which the gold(I) centers make relatively close contact with an Au···Au distance of 3.4615(2) Å. This distance is significantly longer than the corresponding distance (3.1882(1) Å) in [Au{C(NHMe)$_2$}$_2$](PF$_6$)·0.5(acetone), **1**. The Au···Au···Au angle is slightly bent, 169.22(1)°, as seen in the stereoview in Figure 10. Within the stacked cations in [Au{C(NHMe)$_2$}$_2$]-(BF$_4$), **2**, the ligands have an eclipsed orientation rather than the staggered arrangement seen for [Au{C(NHMe)$_2$}$_2$](PF$_6$)·0.5(acetone), **1**. The separation between the planes of the cations is 3.341 Å, which is shorter than the Au···Au distance due to the offset nature of the stacking. As a result of this offset, the

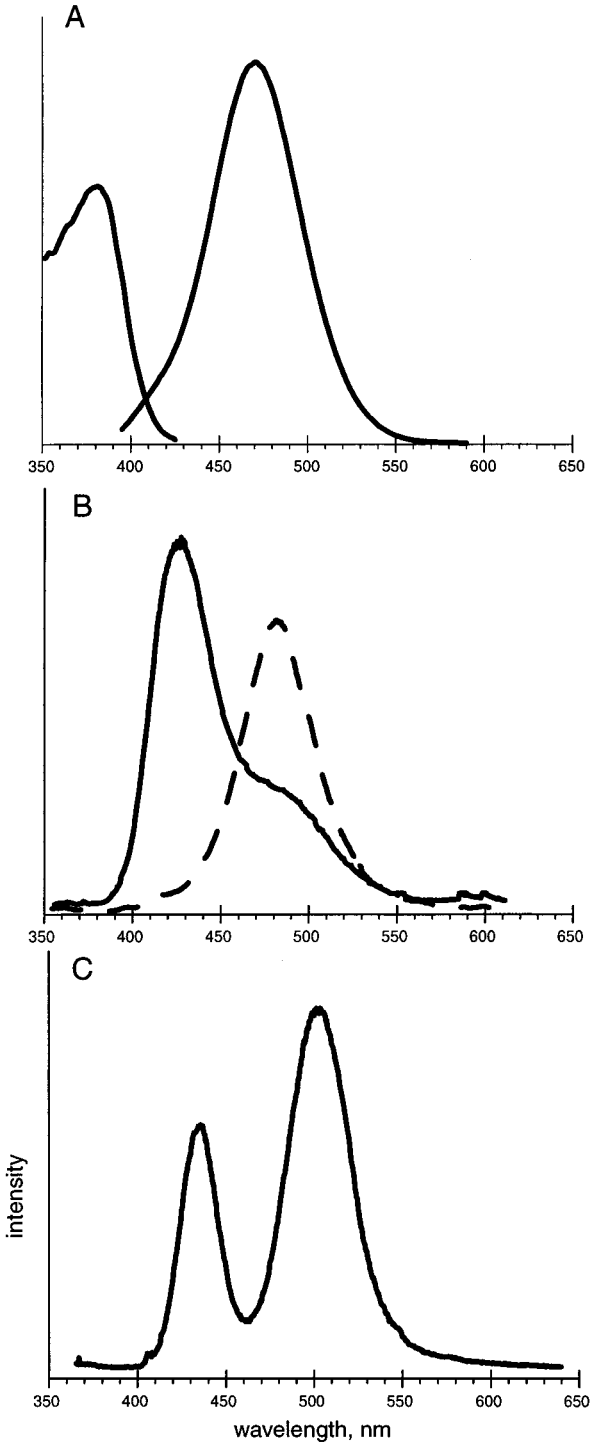

Figure 7. Emission spectra of polycrystalline [Au{C(NHMe)$_2$}$_2$](BF$_4$), **2**. A, Emission ($\lambda_{excitation}$, 383 nm) and excitation ($\lambda_{emission}$, 482 nm) spectra at 300 K. B, Time-resolved emission spectra at 295 K: solid line, emission acquired within 50 ns of a 337 nm laser pulse; dotted line, emission acquired 200 ns after the laser pulse. C, Emission ($\lambda_{excitation}$, 365 nm) spectrum at 77 K.

gold atom of one cation is only 3.561 Å from the carbene carbon atom of an adjoining cation.

Comparison of the structure of [Au{C(NHMe)$_2$}$_2$](BF$_4$), **2**, with that of [Au{C(NH*p*-tolyl)$_2$}$_2$](BF$_4$) is also informative.[38] There are no aurophilic interactions in [Au{C(NH*p*-tolyl)$_2$}$_2$]-

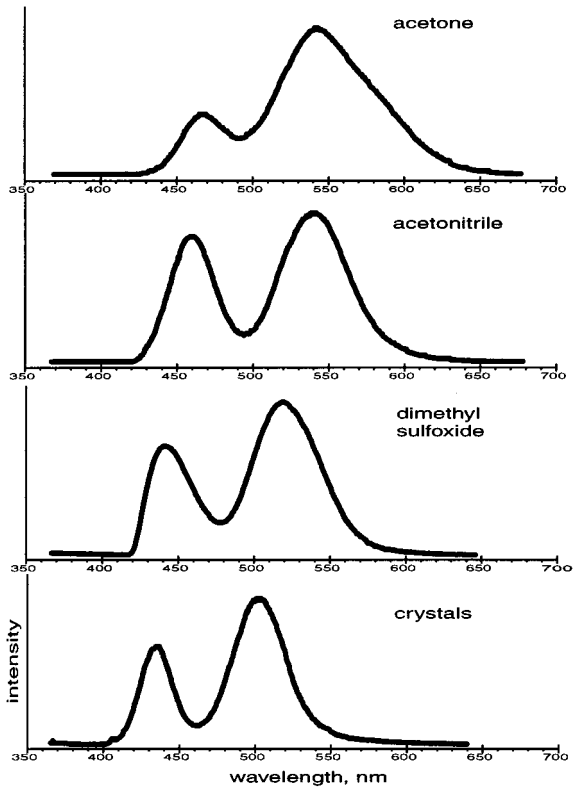

Figure 8. Luminescence spectra obtained from 6 mM solutions of [Au{C(NHMe)$_2$}$_2$](BF$_4$), **2**, acetone, dimethyl sulfoxide, and acetonitrile frozen at 77 K.

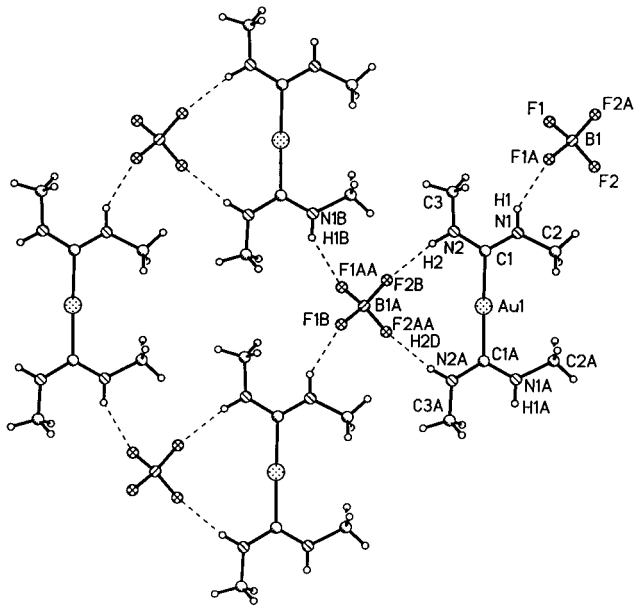

Figure 9. A view of the solid-state structure of [Au{C(NHMe)$_2$}$_2$](BF$_4$), **2**, which emphasizes the hydrogen-bonding interactions between the N−H groups of the cations and the fluorine atoms of the anions.

(BF$_4$); the shortest distance between gold atoms is over 7 Å. The two phenyl rings occupy inner positions in the planar carbene ligands and are twisted out of the plane of the N$_2$AuC units. Thus, they serve to insulate the gold atoms from each other. The two carbene ligands are not coplanar; the dihedral angle between them is 68.1°. The tetrafluoroborate anions are, however, hydrogen bonded to the N−H groups of the carbene ligands. Both N−H groups in one carbene ligand are hydrogen

(38) Banditelli, G.; Bonati, F.; Calogero, S.; Valle, G. *J. Organomet. Chem.* **1984**, *275*, 153.

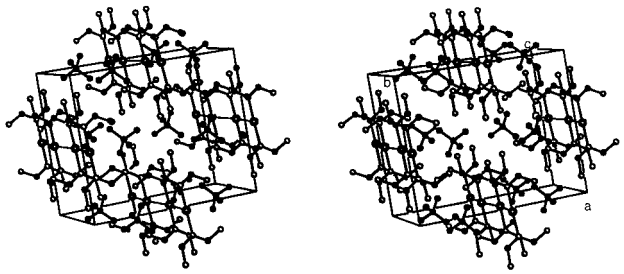

Figure 10. A stereoview of the structure of [Au{C(NHMe)$_2$}$_2$](BF$_4$), **2**.

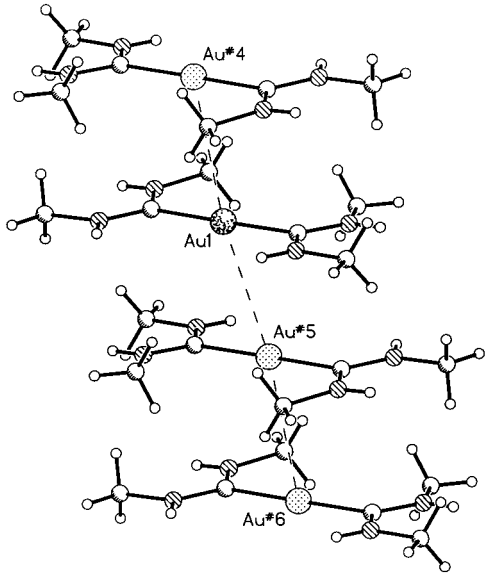

Figure 11. A view of [Au{C(NHMe)$_2$}$_2$](BF$_4$), **2**, which shows the offset nature of the cation stacking.

bonded to two fluorine atoms of a tetrafluoroborate anion, while the other two N−H groups of the other carbene ligand interact with a fluorine atom of a second tetrafluoroborate anion.

Luminescence from [Au{C(NMe$_2$)(NHMe)}$_2$](PF$_6$), 3. Under conditions where [Au{C(NHMe)$_2$}$_2$](PF$_6$)·0.5(acetone), **1**, and [Au{C(NHMe)$_2$}$_2$](BF$_4$), **2**, are strongly luminescent, no luminescence could be detected visually or spectrometrically for this crystalline solid. Similarly, solutions of this complex are not luminescent at room temperature. However, upon freezing at 77 K, the solutions are luminescent as shown in Figure 12. The spectra shown in this figure again consist of two main bands.

Crystal Structure of [Au{C(NMe$_2$)(NHMe)}$_2$](PF$_6$), 3. The structure of [Au{C(NMe$_2$)(NHMe)}$_2$](PF$_6$), **3**, is shown in Figure 13. All of the atoms of the cation with the exception of two hydrogen atoms of each methyl group lie in a crystallographic mirror plane. The phosphorus atom and two of the fluorine atoms of the hexafluorophosphate anion also lie in the same plane. The structure of the cation resembles that of the cation in [Au{C(NHMe)$_2$}$_2$](PF$_6$)·0.5(acetone), **1**, except that a methyl group replaces each of the outer N−H protons. As seen in Table 1, the bond lengths in the cation are similar to those found in the other two salts, [Au{C(NHMe)$_2$}$_2$](PF$_6$)·0.5(acetone), **1**, and [Au{C(NHMe)$_2$}$_2$](BF$_4$), **2**.

Within the planar section shown in Figure 13, there are hydrogen bonds between the N−H group of the cation and two equivalent fluorine atoms of the hexafluorophosphate anion. The H(2)···F(1) distance is 2.37(4), and the N(2)···F(1) distance is

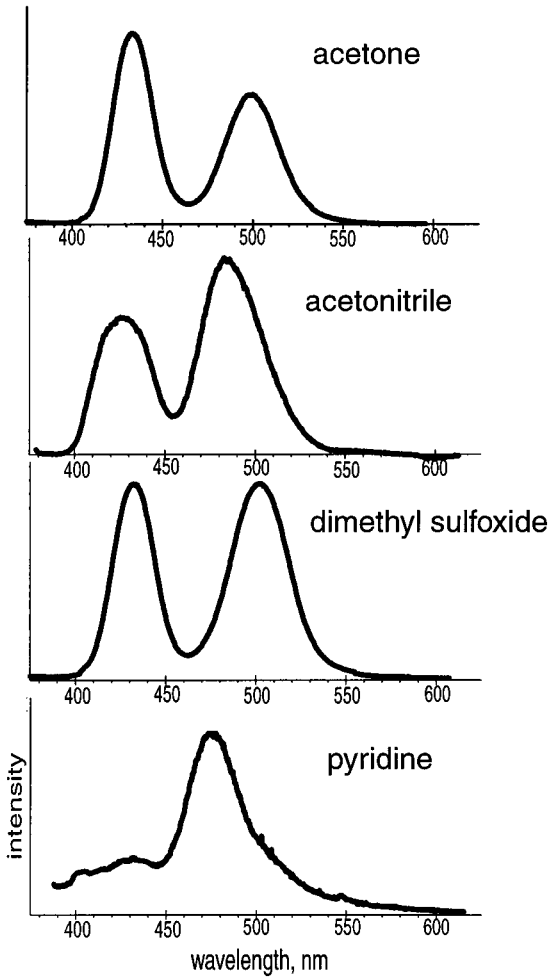

Figure 12. Luminescence spectra obtained from 6 mM solutions of [Au{C(NMe$_2$)(NHMe)}$_2$](PF$_6$), **3**, in acetone, acetonitrile, dimethyl sulfoxide, and pyridine solutions frozen at 77 K.

3.110(3) Å. Additionally, there is a C−H···F bond between one of the hydrogen atoms of the inner methyl group of the carbene ligand and a fluorine atom of the hexafluorophosphate anion. The H(3B)···F(2) distance is 2.547(4), and the C(3)···F(2) distance is 3.477(3) Å.

There are no aurophilic interactions between the cations in this solid. The shortest distance between gold ions is 7.1109(3) Å. Thus, the introduction of the added methyl group into this carbene ligand inhibits the hydrogen-bonding scheme shown in Figure 4. Consequently, the hydrogen bonding available in [Au{C(NMe$_2$)(NHMe)}$_2$](PF$_6$), **3**, does not promote an aurophilic interaction between cations.

Discussion

The structural data reported here demonstrate that the cation [Au{C(NHMe)$_2$}$_2$]$^+$ can participate in self-association through aurophilic interactions. It is significant to note that the aurophilic attraction can overcome the Coulombic factors which should serve to separate the cations from each other. In these salts the mode of self-association depends on the anion present. Thus, in [Au{C(NHMe)$_2$}$_2$](PF$_6$)·0.5(acetone), **1**, the cations form linear stacks with shortened Au···Au contacts (the Au···Au distance is 3.1882(1) Å), while in [Au{C(NHMe)$_2$}$_2$](BF$_4$), **2**, the cations form offset stacks with longer Au···Au distances (3.4615(2) Å). In [Au{C(NHMe)$_2$}$_2$](PF$_6$)·0.5(acetone), **1**, the

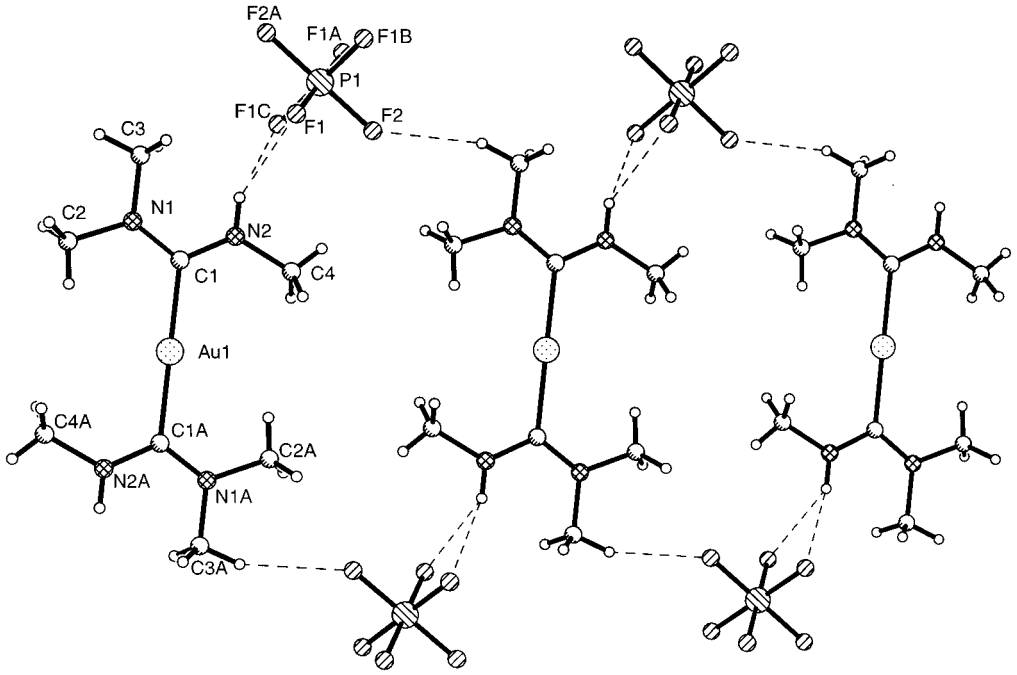

Figure 13. A view of the structure of $[Au\{C(NMe_2)(NHMe)\}_2](PF_6)$ looking down on the plane of the cations. The closest Au to Au contact is 7.1109(3) Å.

ligands are in staggered orientations, while in $[Au\{C(NHMe)_2\}_2](BF_4)$, **2**, they are eclipsed but offset.

With hexafluorophosphate and tetrafluoroborate as the counterions in these salts, hydrogen bonding with the ligands is an important factor directing the solid-state structure. Thus, in $[Au\{C(NHMe)_2\}_2](PF_6)\cdot 0.5$(acetone), **1**, the hexafluorophosphate anions interact directly with adjacent cations within a column and serve to counterbalance the charge buildup in the column of gold cations. This hydrogen bonding in part facilitates the shortened Au···Au contact seen in the hexafluorophosphate salt. We anticipate that other anions will produce different modes of self-association of $[Au\{C(NHMe)_2\}_2]^+$ and related cations. For example, the cation $[Au\{C(OMe)(NHMe)\}_2]^+$ has been found to exist as a monomer, a dimer (with an Au···Au distance of 3.1955(3) Å), and a trimer (with an Au···Au distance of 3.27797(15) Å) in three different salts that have been examined crystallographically.[37] For $[Au\{C(NHMe)_2\}_2]^+$ this issue is under investigation in this laboratory.

The formation of extended chains of Au(I) complexes through aurophilic interactions is relatively uncommon. Generally, the aurophilic interactions between monomeric, two-coordinate gold(I) complexes lead to simple dimerization. However, in the solid state $\{(Me_2S)AuCl\}_n$ has an extended chain structure with an Au···Au distance of 3.226(1) Å and an Au···Au···Au angle of 168.1(1)°,[39] and $\{(2\text{-picoline})AuCl\}_n$ forms a similar chain with an Au···Au distance of 3.1960(4) Å and an Au···Au···Au angle of 165.079(12)°.[40] Notice that in these chains, which involve neutral molecules, the Au···Au separations are longer than that in $[Au\{C(NHMe)_2\}_2](PF_6)\cdot 0.5$(acetone), **1** (3.1882(1) Å,), where cations self-associate. The Au···Au separations are even larger in $(C_{12}H_{14}N_2)[Au_2I_4]$, where a set of $[AuI_2]^-$ anions self-associates through aurophilic attraction with a Au···Au distance of 3.3767(3) Å.[41] However, in $[(3\text{-picoline})_2Au][AuCl_2]$, where cations and anions associate into zigzagged chains, the Au···Au separation is somewhat shorter, 3.1538(12) Å,[39] and in $[(tetrahydrothiophene)_2Au][AuI_2]$ the Au···Au distances are very short, 2.967(2) and 2.980(2) Å.[42]

The luminescence observed from the solids, $[Au\{C(NHMe)_2\}_2](PF_6)\cdot 0.5$(acetone), **1**, and $[Au\{C(NHMe)_2\}_2](BF_4)$, **2**, along with the luminescence from frozen solutions of these complexes appears to result from the self-association of the cations through aurophilic interactions. Thus, the $[Au\{C(NHMe)_2\}_2]^+$ cation is not luminescent in solution, where we presume it is monomeric, and $[Au\{C(NMe_2)(NHMe)\}_2](PF_6)$, **3**, is nonluminescent in solution and in the solid state, where it is also monomeric and unaffected by aurophilic interactions. Within the chains of gold atoms, overlap of the occupied $5d_{z^2}$ orbitals (where z is the axis defined by the Au···Au···Au chain) on gold will produce a filled band of orbitals, while overlap of the empty $6p_z$ gold orbitals will produce a corresponding band of unoccupied orbitals. The spectroscopic features seen for $[Au\{C(NHMe)_2\}_2](PF_6)\cdot 0.5$(acetone), **1**, and $[Au\{C(NHMe)_2\}_2](BF_4)$, **2**, in the solid state result from excitation of electrons from the filled $5d_{z^2}$ band to the empty $6p_z$ band. The red shifts of the emission maxima in $[Au\{C(NHMe)_2\}_2](PF_6)\cdot 0.5$(acetone), **1**, relative to $[Au\{C(NHMe)_2\}_2](BF_4)$, **2**, indicate a greater orbital interaction in the hexafluorophosphate salt **1** consistent with its shorter Au···Au distance. The fact that the excitation profiles for the solids (see Figure 1) do not correspond to the absorption spectrum obtained from solution of these complexes (with λ_{max} of 210 nm) indicates that supramolecular interactions (aurophilic attractions) are responsible for the luminescence.

The observation that the emission spectra obtained from frozen dilute solutions of $[Au\{C(NHMe)_2\}_2](PF_6)\cdot 0.5$(acetone), **1**, seen in Figure 4, strongly resemble the spectra obtained from polycrystalline $[Au\{C(NHMe)_2\}_2](PF_6)\cdot 0.5$(acetone), **1**, suggests

(39) Jones, P. G.; Lautner, J. *Acta Crystallogr., Sect. C* **1988**, *44*, 2089.
(40) Jones, P. G.; Ahrens, B. *Z. Naturforsch.* **1998**, *53b*, 653.
(41) Tang, Z.; Litvinchuk, A. P.; Lee, H.-G.; Guloy, A. M. *Inorg. Chem.* **1998**, *37*, 4752.
(42) Ahrland, S.; Norén, B.; Oskarsson, Å. *Inorg. Chem.* **1985**, *24*, 1330.

that similar emitting entities are present. Indeed it is entirely reasonable that an oligomeric form of [Au{C(NHMe)$_2$}$_2$](PF$_6$) with a structure analogous to that of [Au{C(NHMe)$_2$}$_2$](PF$_6$)·0.5(acetone), **1**, crystallizes from solution during the freezing process. In this regard, crystallization of various solvates with the solvent molecules occupying the sites occupied by the acetone molecules in crystalline [Au{C(NHMe)$_2$}$_2$](PF$_6$)·0.5-(acetone), **1** (as seen in Figure 6), is a realistic possibility. During the freezing process, the solvent solidifies, and the concentration of the solute in the remaining unfrozen solvent increases. The novel aspects of reactions occurring in freezing solvents have been reviewed previously.[43] The concentration of the solute during the freezing facilitates aggregation of the gold(I) cations and the formation of species similar in structure to the arrangement seen in crystalline [Au{C(NHMe)$_2$}$_2$](PF$_6$)·0.5-(acetone), **1**. Similarly the emission spectra seen for the frozen solution of [Au{C(NHMe)$_2$}$_2$](BF$_4$), **2**, as shown in Figure 8, resemble the emission spectra from crystalline [Au{C(NHMe)$_2$}$_2$]-(BF$_4$), **2**. Again, we propose that self-association through aurophilic attractions is responsible for the emission and that similar structures are found in the solid and in the frozen samples, where [Au{C(NHMe)$_2$}$_2$](BF$_4$), **2**, may crystallize. The emission spectra of frozen solutions of [Au{C(NMe$_2$)(NHMe)}$_2$]-(PF$_6$), **3**, are similar to those of the other salts. This suggests that aggregates (dimers, trimers, higher oligomers) of cations also are responsible for the luminescence seen from frozen solutions of [Au{C(NMe$_2$)(NHMe)}$_2$](PF$_6$), **3**. Interestingly, these proposed aggregates do not occur in crystals of [Au-{C(NMe$_2$)(NHMe)}$_2$](PF$_6$), **3**. Thus, the freezing process must facilitate the formation of these aggregates. The emission bands of [Au{C(NMe$_2$)(NHMe)}$_2$](PF$_6$), **3**, in frozen solution are generally at higher energies than those of **1** and **2**. This indicated a smaller interaction of the overlapping gold orbitals and a greater Au···Au distance in the aggregates formed by [Au-{C(NMe$_2$)(NHMe)}$_2$](PF$_6$), **3**. Although the [Au{C(NMe$_2$)-(NHMe)}$_2$]$^+$ cations do not self-associate in crystalline [Au-{C(NMe$_2$)(NHMe)}$_2$](PF$_6$), **3**, this cation is planar, and there is no steric barrier to self-association.

The observations that the remarkable range of colors seen in Figure 2 depends on the concentration of [Au{C(NHMe)$_2$}$_2$]-(PF$_6$)·0.5(acetone), **1**, in the initial solution also substantiates the proposition that aggregation is crucial in creating the luminescence that is responsible for this range of colors. Hence, we propose that the freezing process results in the formation of an array of aggregated cations whose structures differ from that seen in solid [Au{C(NHMe)$_2$}$_2$](PF$_6$)·0.5(acetone), **1**. The formation of such aggregates is favored in the most concentrated solutions we have examined and is further promoted by the fact that freezing of the solution results in further concentration of the solute.

The aggregation of cations observed here is related to observations made on {Au(S$_2$CN(C$_5$H$_{11}$)$_2$}$_2$.[22] This dimer crystallizes as an orange, luminescent form from dimethyl sulfoxide. In this form the dimers (with an intramolecular Au···Au distance of 2.7690(7) Å) associate through further intermolecular Au···Au contacts with a separation of 2.9617-(7) Å into extended chains. In contrast, when crystallized from *n*-propanol/benzene {Au(S$_2$CN(C$_5$H$_{11}$)$_2$}$_2$ forms colorless crystals in which the shortest intermolecular Au···Au contact is over 8 Å long. A counterpart to the aggregation phenomena involving [Au{C(NHMe)$_2$}$_2$](PF$_6$)·0.5(acetone), **1**, in an anionic system is seen in the behavior of [Au(CN)$_2$]$^-$ and [Ag(CN)$_2$]$^-$ which also forms oligomers with varying luminescence properties in solution.[44]

Structural factors which may contribute to the variation in luminescence behavior of these complexes include the number of gold(I) ions involved in specific aggregates, the distance between the gold(I) ions within an aggregate, the relative orientation of the carbene ligands (which may run from little direct overlap in the staggered arrangement to maximal overlap in the eclipsed arrangement), hydrogen-bonding interactions of the cation with the anion and hence the specific identity of the anion, hydrogen-bonding interactions of the cation with the solvent, and coordination of the solvent to the gold(I) ions in the aggregates. Additionally, the freezing process may create an array of specific aggregates that may differ particularly in the number of gold(I) ions involved but may also differ in any of the other structural factors listed above. Solvent molecules may cap the aggregates and constrain their sizes by coordination or by hydrogen bonding with the ligands. Further work is clearly needed to understand the range of aggregates that these gold complexes can form and the conditions necessary for their formation. Understanding these aspects should allow the remarkable luminescence feature shown here to be developed into sensors for a range of chemical environments.

Experimental Section

Materials. Literature procedures were used for preparation of methyl isocyanide,[45,46] [Au{C(NHMe)$_2$}$_2$](PF$_6$)·0.5(acetone),[32] and [Au{C(NMe$_2$)-(NHMe)}$_2$](PF$_6$), **3**.[32]

[Au{C(NHMe)$_2$}$_2$](BF$_4$), 2. Methyl isocyanide (0.20 mL, 4 mmol) was added at room temperature to an orange solution of hydrogen tetrachloroaurate(III) hydrate (0.27 g, 0.8 mmol) in water (10 mL). The reaction mixture immediately turned yellow, and a yellow precipitate formed during the addition. With continued stirring, the initial precipitate redissolved. A 1.50 mL (1.7 mmol) portion of 40% aqueous methylamine was added to the yellow solution, and the mixture was stirred for one-half of an hour. The colorless crystalline product formed after the addition of a saturated methanolic solution of tetrabutylammonium tetrafluoroborate. The material was collected and purified by recrystallization from acetone with diffusion of ethyl ether, affording 0.32 g (81% yield) of colorless, crystalline [Au{C(NHMe)$_2$}$_2$]-(BF$_4$), **2**. [Au{C(NHMe)$_2$}$_2$](BF$_4$), **2**, is not soluble in chloroform or dichloromethane, but soluble in acetonitrile, acetone, dimethyl sulfoxide, dimethyl formamide, and pyridine. ^{1}H NMR (300.1 MHz, 298 K, CD$_3$-CN): δ 6.92 (2H, br), 3.16 (3H, d), 2.65 (3H, d) ppm. IR (KBr pellet cm^{-1}): 3455 (s), 3393 (s), 3271 (m), 3055 (w), 2950 (m), 2851 (w), 1592 (vs), 1526 (s), 1452 (w), 1369 (w), 1313 (w), 1194 (w), 1029 (m), 878 (bs), 850 (vs), 687 (w), 608 (m), 559 (s).

Physical Measurements. ^{1}H NMR spectra were recorded for chloroform-*d* solutions on a General Electric QE-300 NMR spectrometer operating at 300 MHz with an external tetramethylsilane standard and the high-field positive convention for chemical shifts. Infrared spectra were recorded as pressed KBr pellets on a Matteson Galaxie Series FTIR 3000 spectrometer. Electronic absorption spectra were recorded using a Hewlett-Packard 8450A diode array spectrophotometer. Conventional fluorescence excitation and emission spectra were

(43) Pincock, R. E. *Acc. Chem. Res.* **1969**, *2*, 97.

(44) Rawashdeh-Omary, M. A.; Omary, M. A.; Patterson, H. H.; Fackler, J. P., Jr. *J. Am. Chem. Soc.* **2001**, *123*, 11237.

(45) Weber, W. P.; Gokel, G. W.; Ugi, I. K. *Angew. Chem., Int. Ed. Engl.* **1972**, *11*, 530.

(46) Gokel, G. W.; Widera, R. P.; Weber, W. P. *Org. Synth.* **1976**, *55*, 96.

Table 2. Crystallographic Data for Compounds **1**−**3**[a]

	[Au{C(NHMe)$_2$}$_2$](PF$_6$)·0.5(acetone), **1**	[Au{C(NHMe)$_2$}$_2$](BF$_4$), **2**	[Au{C(NMe$_2$)(NHMe)}$_2$](PF$_6$), **3**
formula	$C_{7.5}H_{19}AuF_6N_4O_{0.5}P$	$C_6H_{16}AuBF_4N_4$	$C_8H_{20}AuF_6N_4P$
fw	515.20	428.00	514.22
a, Å	15.4419(6)	11.9132(7)	12.2551(6)
b, Å	15.4419(6)	14.6089(9)	7.2162(4)
c, Å	6.3764(2)	6.8923(4)	8.5987(4)
α, deg	90	90	90
β, deg	90	94.5880(10)	98.4280(10)
γ, deg	90	90	90
V, Å^3	1520.47(10)	1195.68(12)	752.22(7)
Z	4	4	2
cryst syst	tetragonal	monoclinic	monoclinic
space group	$P4_2/mnm$	$C2/c$	$C2/m$
T, K	90(2)	90(2)	90(2)
λ, Å	0.71073	0.71073	0.71073
ρ, g/cm^3	2.251	2.378	2.270
μ, mm^{-1}	9.842	12.334	9.944
R_1 (obsd data)	0.016	0.015	0.014
wR2 (all data, F^2 refinement)	0.041	0.036	0.035

[a] $R1 = \sum||F_o| - |F_c||/\sum|F_o|$; $wR2 = [\sum[w(F_o^2 - F_c^2)^2]/\sum[w(F_o^2)^2]]^{1/2}$.

recorded on a Perkin-Elmer LS50B luminescence spectrophotometer. Additional emission spectra were excited with a filtered 100 W Hg lamp and recorded with a 1 m Czerny-Turner spectrometer. The spectra are uncorrected for spectrometer sensitivity. Decay measurements used a N_2 laser (337 nm) for excitation and the 1 m spectrometer to monitor the emission intensity. The decay data were collected with a digital oscilloscope and analyzed with a least-squares algorithm.

X-ray Crystallography and Data Collection. The crystals were removed from the glass tubes in which they were grown together with a small amount of mother liquor and immediately coated with a hydrocarbon oil on the microscope slide. Suitable crystals were mounted on glass fibers with silicone grease and placed in the cold stream of a Bruker SMART CCD with graphite monochromated Mo Kα radiation at 90(2) K. Check reflections were stable throughout data collection. Crystal data are given in Table 2.

The structures were solved by Patterson methods and refined using all data (based on F^2) using the software of SHELXTL 5.1. A semiempirical method utilizing equivalents was employed to correct for absorption.[47] Hydrogen atoms were added geometrically and refined with a riding model.

Acknowledgment. We thank the Petroleum Research Fund (grant 37056-AC) and the National Science Foundation (grant CHE 9610507 and CHE 0070291) for support. The Bruker SMART 1000 diffractometer was funded in part by NSF Instrumentation grant CHE 9808259.

Supporting Information Available: X-ray crystallographic files for [Au{C(NHMe)$_2$}$_2$](PF$_6$)·0.5(acetone), **1**, [Au{C(NHMe)$_2$}$_2$](BF$_4$), **2**, and [Au{C(NMe$_2$)(NHMe)}$_2$](PF$_6$), **3** (CIF). This material is available free of charge via the Internet at http://pubs.acs.org.

JA012397S

(47) SADABS 2.0, Sheldrick, G. M. Based on a method of Blessing, R. H. *Acta Crystallogr., Sect. A* **1995**, *51*, 33.